Thermal Isomerisation of Tris(silyl)hydroxylamines to Silylaminodisiloxanes – Experimental and Quantum Chemical Results

Stefan Schmatz,*[a] Friedhelm Diedrich,[b] Christina Ebker,[b] and Uwe Klingebiel*[b]

Keywords: Silicon / Hydroxylamines / Isomerisation / Ab initio calculations / Transition states

O-Lithio-*N*,*N*-bis(trimethylsilyl)hydroxylamide, LiO–N-$(SiMe_3)_2$, reacts with $ClSiMe_2H$ to give $HMe_2Si–O–N(SiMe_3)_2$ (**1**), while $LiO–N(SiMe_2CMe_3)_2$ reacts with $C_6H_5SiF_3$ to give $C_6H_5SiF_2–O–N(SiMe_2CMe_3)_2$ (**2**). **2** isomerises in solution to give *N*,*O*-bis(*tert*-butyldimethylsilyl)-*N*-[difluoro(phenyl)silyl]hydroxylamine (**3**). Boiling of **1** leads to the structurally isomeric silylaminodisiloxane, $Me_3Si–O–SiMe_2–NH–SiMe_3$ (**4**), while boiling of **3** leads to the isomeric $Me_3CSiMe_2–O–Si(Me)CMe_3–NMe–SiF_2C_6H_5$ (**5**). Quantum chemical calculations (B3LYP) on the thermal rearrangement of tris(silyl)hydroxylamines to silylaminodisiloxanes for the model compounds $H_3Si–O–N(SiMe_3)_2$ (**A**), $Me_3Si–O–N(SiH_3)_2$ (**B**), $Me_3Si–O–N(SiH_3)SiMe_2F$ (**C**), and $Me_3Si–O–N(SiMe_2F)SiMeF_2$ (**D**) demonstrate that *N*-bonded silyl units, e.g. SiH_2 in model compound **B** or SiFMe in model compound **D**, preferentially insert into the N–O bond. The reaction mechanisms and the structures of the transition states are discussed in detail.
(© Wiley-VCH Verlag GmbH, 69451 Weinheim, Germany, 2002)

Introduction

The most dramatic difference between the chemistry of silylhydroxylamines and that of organylhydroxylamines is the ability of the former to undergo anionic, radical, and thermal intramolecular rearrangements.[1–7] The first example of a 1,2-anionic rearrangement of a silyl group from an oxygen atom to a nitrogen atom was observed for lithiated *N*,*O*-bis(silyl)hydroxylamines.[1,2,8] Although lithiobis(silyl)hydroxylamines have been successfully used in the synthesis of tris(silyl)hydroxylamines since the end of the 1960s, the first crystal structures of these compounds were described only two years ago.[6,7] It was found that lithium derivatives of *N*,*O*-bis(silyl)hydroxylamines form *O*-lithio-*N*,*N*-bis(silyl)hydroxylamides in the solid state.

Depending on the bulkiness of the silyl groups and on the solvent used, $(Li–O)_{2,3,4}$ four-, six-, or eight-membered rings were formed,[6,7] and dimeric, trimeric, or tetrameric *O*-lithio-*N*,*N*-bis(silyl)hydroxylamides could be isolated. This indicated that silyl group migration from the oxygen atom to the nitrogen atom had occurred. In the reactions of halosilanes with these lithium salts, the new silyl group is attached to the oxygen atom in each case [Equation (1)].

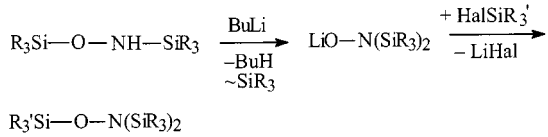

(1)

R, R' = alkyl, aryl

1,2-Silyl shifts in *neutral* organosilylhydroxylamines have been known since 1973,[1,2,9] when Frainnet and Nowakowski described an exchange of trialkylsilyl groups in bis(organosilyl)hydroxylamines.[9] Later, West and co-workers found a reversible rearrangement involving positional exchange between the organosilicon groups on the oxygen and the nitrogen atom in tris(silyl)hydroxylamines, which they suggested to proceed via a dyotropic transition state[1,2,10,11] [Equation (2)].

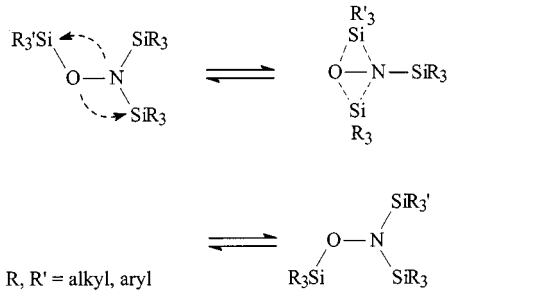

(2)

R, R' = alkyl, aryl

In 1998, we studied the rearrangement of *O*-(fluorosilyl)-*N*,*N*-bis(trimethylsilyl)hydroxylamines to the isomeric *N*-

[a] Institut für Physikalische Chemie der Universität Göttingen, Tammannstraße 6, 37077 Göttingen, Germany
E-mail: sschmat@gwdg.de
[b] Institut für Anorganische Chemie der Universität Göttingen, Tammannstraße 4, 37077 Göttingen, Germany
E-mail: uklinge@gwdg.de

(fluorosilyl)-*N*,*O*-bis(trimethylsilyl)hydroxylamines and found it to be irreversible.[5] Ab initio and density functional calculations were consistent with the dyotropic course of the isomerisation.

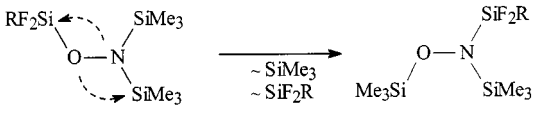

(3)

R = alkyl, aryl

In a thermal rearrangement, which proceeds at temperatures up to 200 °C, tris(organosilyl)hydroxylamines undergo an intramolecular isomerisation involving the insertion of a silicon moiety into the bond between the nitrogen and the oxygen atom and the transfer of an organyl group from the silicon to the nitrogen atom, thereby forming silylaminodisiloxanes.[1,2,6,12]

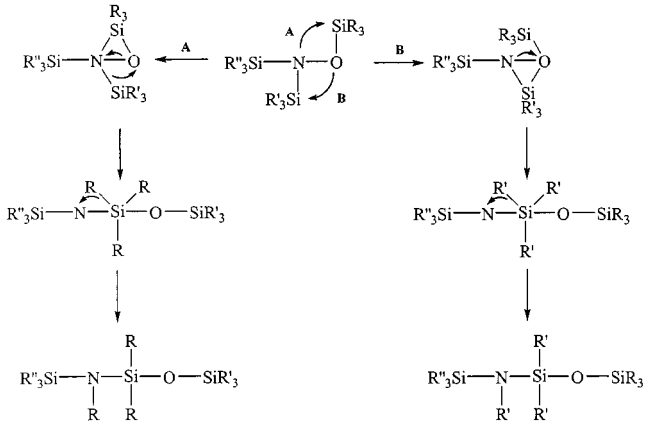

(4)

This conversion occurs in high yields. We studied rearrangements of *N*-(fluorosilyl)-*N*,*O*-bis(organylsilyl)hydroxylamines and found that the insertion of a silicon moiety into the N−O bond exclusively involves the silicon moiety that was bonded to the nitrogen atom. The insertion of an SiF_2 unit into the N−O bond has not been observed.

For a better understanding of our results, we report herein on quantum chemical investigations of the isomerisations of tris(silyl)hydroxylamines based on several model compounds and the thermal rearrangements of two *N*,*N*,*O*-tris(silyl)hydroxylamines with formation of the isomeric silylaminodisiloxanes.

Results and Discussion

Experimental

O-Lithio-*N*,*N*-bis(trimethylsilyl)hydroxylamide reacts with $ClSiMe_2H$ to give *O*-(dimethylsilyl)-*N*,*N*-bis(trimethylsilyl)hydroxylamine (**1**) [Equation (5)].

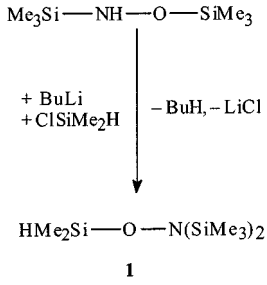

(5)

The lithium salt of *N*,*O*-bis(*tert*-butyldimethylsilyl)hydroxylamine crystallises from THF as dimeric *N*,*N*-bis(*tert*-butyldimethylsilyl)hydroxylamide[7] and reacts with trifluoro(phenyl)silane at 0 °C with formation of *N*,*N*-bis(*tert*-butyldimethylsilyl)-*O*-[difluoro(phenyl)silyl]hydroxylamine (**2**).

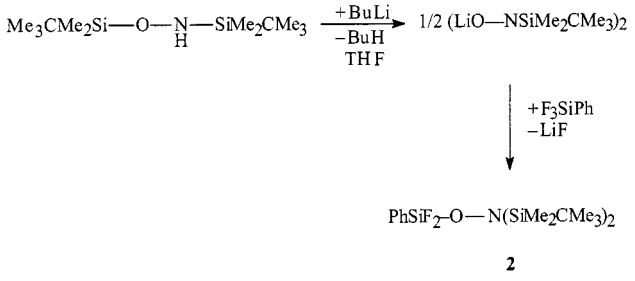

(6)

Product **2** could be isolated following the removal of LiF in a centrifuge by virtue of the low reaction temperature and the bulky $SiMe_2CMe_3$ groups. In solution, even at room temperature, the onset of the dyotropic rearrangement of **2** into the isomeric *N*,*O*-bis(*tert*-butyldimethylsilyl)-*N*-difluorophenylsilyl)hydroxylamine (**3**) can be observed by means of NMR spectroscopy. The conversion of **2** to **3** is found to be quantitative within a few hours in boiling THF. The softer Lewis acid F_2SiPh migrates to the softer Lewis base nitrogen, while the harder Lewis acid $SiMe_2CMe_3$ migrates to the harder Lewis base oxygen.

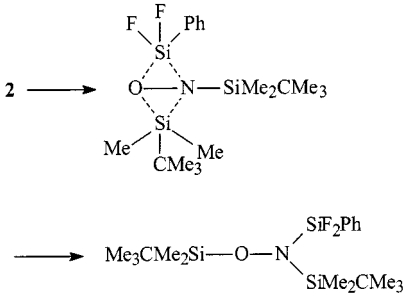

(7)

When heated under reflux for 3 d, **1** and **3** undergo a thermal rearrangement to form the silylaminodisiloxanes **4** and **5**, respectively. The conversion of **1** to **4** was monitored by ^1H NMR spectroscopy. It was found that a structural isomer of **1**, namely *N*-(dimethylsilyl)-*N*,*O*-bis(trimethylsilyl)hydroxylamine, was formed initially, which could not be isolated under the given reaction conditions.

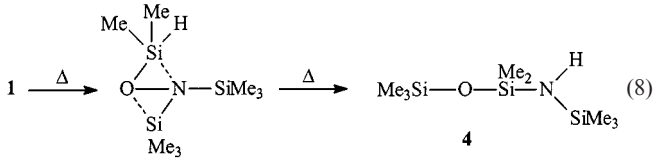

(8)

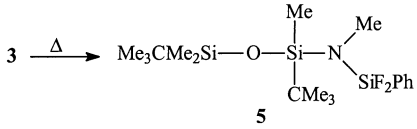

(9)

The formation of **4** involves the insertion of an $SiMe_2$ moiety into the N−O bond and a hydrogen atom transfer from the silicon to the nitrogen atom, whereas the formation of **5** involves the insertion of an $SiMeCMe_3$ moiety into the N−O bond and the migration of a CH_3 group from the silicon to the nitrogen atom.

Quantum Chemical Study on the Isomerisation of Tris(silyl)hydroxylamines

In order to gain more insight into the mechanisms governing the thermal isomerisation reactions of tris(silyl)hydroxylamines, quantum chemical calculations have been carried out.

Methodology

The program package GAUSSIAN-98[13] was employed throughout. The geometries of the minima and first-order saddle points on the potential energy surfaces (PES) were calculated using the density functional variant B3LYP, which is a hybrid method employing Becke's exchange functional[14] and the Lee, Yang, and Parr correlation functional.[15] The 6-31G* basis set was used. The calculated stationary points on the PES were characterised by the Hessian matrices. The obtained harmonic vibrational frequencies were used to calculate the zero-point energy contributions. The saddle points were further characterised using the TS routine in GAUSSIAN-98 (intrinsic reaction coordinate method).[16]

Using the B3LYP/6-31G* methodology, we have recently studied various isomerisation reactions in silylhydrazine chemistry.[17−21] The calculated structures were compared with available X-ray diffraction data and good agreement was found throughout.

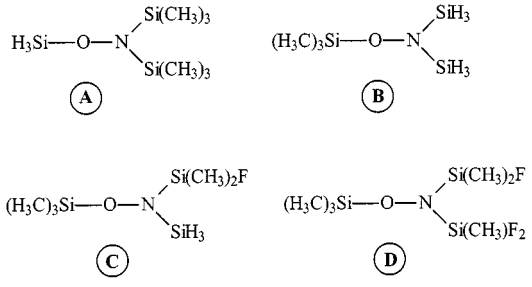

Here, four different model compounds are investigated in detail: *N*,*N*-bis(trimethylsilyl)-*O*-(silyl)hydroxylamine (**A**), *N*,*N*-bis(silyl)-*O*-(trimethylsilyl)hydroxylamine (**B**), *N*-(fluorodimethylsilyl)-*N*-silyl-*O*-(trimethylsilyl)hydroxylamine (**C**), and *N*-(fluorodimethylsilyl)-*N*-(difluoromethylsilyl)-*O*-(trimethylsilyl)hydroxylamine (**D**).

In all four cases, insertion of a silicon atom initially located at the nitrogen atom into the N−O bond occurs. For **A** and **B**, only one product (**PA** and **PB**, respectively) is possible for symmetry reasons. However, **A** and **B** can undergo a dyotropic rearrangement yielding structures **A1** and **B1**. Starting from these isomers, a silicon atom from the nitrogen site can be inserted into the N−O bond yielding products **PA1** and **PB1**, respectively.

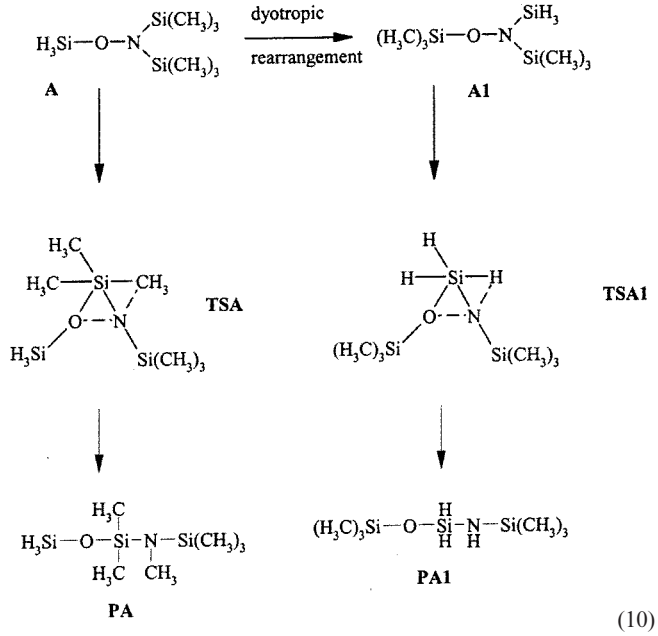

(10)

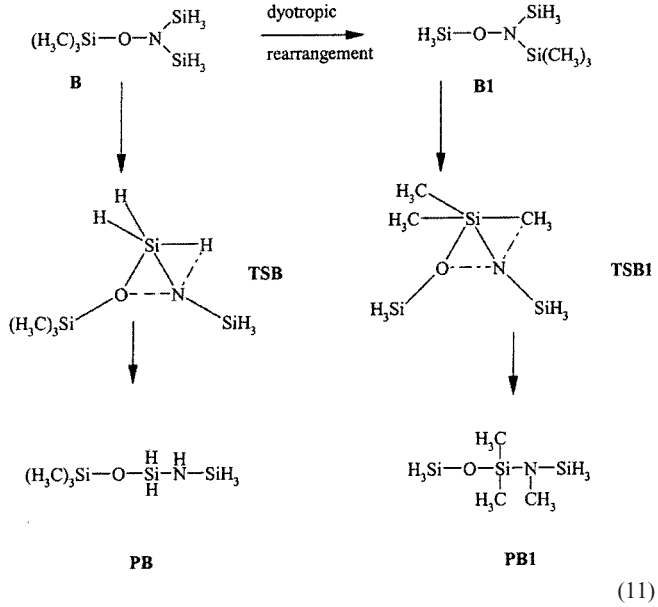

(11)

For **C** and **D**, two different reaction pathways are possible, yielding products **PC1/PC2** and **PD1/PD2**, respectively.

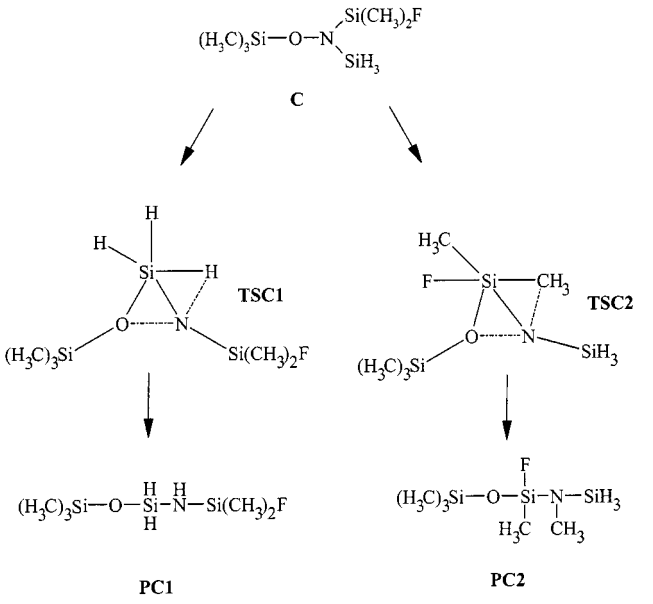

(12)

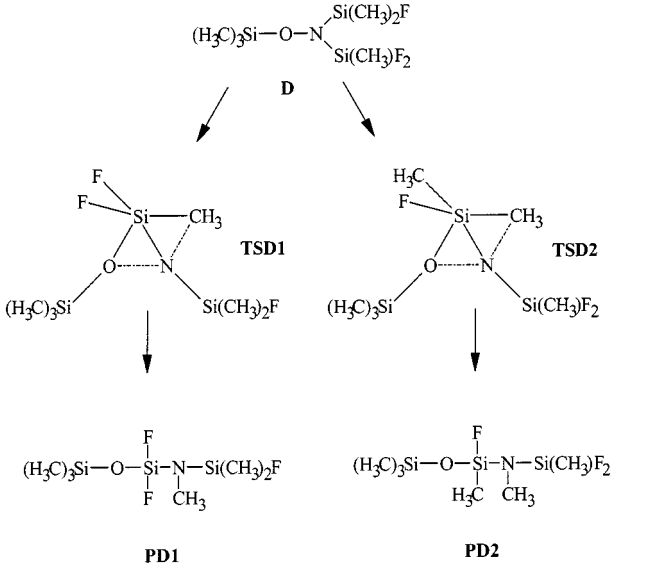

(13)

The transition states corresponding to these reactions are denoted as follows: **TSdA** and **TSdB** are the dyotropic transition states in the isomerisations **A** → **TSdA** → **A1** and **B** → **TSdB** → **B1**. The transition states leading to the silylaminodisiloxanes **PA**, **PA1**, **PB**, **PB1**, **PC1**, **PC2**, **PD1**, and **PD2** are denoted by **TSA**, **TSA1**, **TSB**, **TSB1**, **TSC1**, **TSC2**, **TSD1**, and **TSD2**, respectively.

Structures

In Table 1, the B3LYP/6-31G* equilibrium geometries for the hydroxylamines **A**, **A1**, **B**, **B1**, **C**, and **D** are given. **A** and **B** exhibit C_s symmetry with the Si−O−N chain contained in the symmetry plane. The O−N bond length is calculated to be within the range 147−150 pm. Electron-withdrawing (e.g. fluorosilyl) groups shorten the O−N bond. Depending on the substituents at the silicon atom, the Si−O bond lengths range from 169 to 172 pm and the Si−N bond lengths from 173 to 179 pm. The Si−O−N angles are in the range 109 to 118°, indicating pure sp^3 to sp^2 hybridisation of the oxygen atom. The angles O−N−Si, on the other hand, clearly show that the nitrogen atom is sp^3-hybridised. Depending on the steric demand of the silyl groups, the Si−N−Si angles are between 122 and 129°. As can be seen from the torsional angles Si−O−N−Si, all hydroxylamines adopt a *trans* conformation.

Table 1. B3LYP/6-31G(d) equilibrium geometries of the tris(silyl)hydroxylamines (reactants **A**, **A1**, **B**, **B1**, **C**, and **D**); bond lengths in pm, angles in °; bond angles are denoted by α, torsional angles by θ; **A** and **B** exhibit C_s symmetry; values in parentheses give the equilibrium geometry of structure **B** obtained at the B3LYP/6-31+G(d) level of theory; **C**: Si′ = $SiMe_2F$; **D**: Si′ = $SiMeF_2$

	A	**A1**	**B**	**B1**	**C**	**D**
r(SiO)	168.5	170.8	171.3 (171.7)	169.0	170.9	172.0
r(ON)	149.8	148.4	147.7 (147.6)	149.2	147.6	146.6
r(NSi′)	178.8	176.0	176.1 (176.4)	178.9	176.2	173.1
r(NSi′′)	178.8	178.8	176.1 (176.4)	176.1	176.6	175.7
α(SiON)	110.2	117.0	114.8 (115.0)	108.5	116.2	117.6
α(ONSi′)	105.4	107.7	108.2 (108.2)	108.6	111.2	108.4
α(Si′NSi′′)	127.5	123.4	125.0 (125.1)	126.9	122.2	128.9
θ(SiONSi′)	111.0	121.9	111.0 (110.9)	115.2	118.4	117.4

The geometries of the two saddle points corresponding to the dyotropic transition states **TSdA** and **TSdB** are given in Table 2. The structure of **TSdB** is shown graphically in Figure 1. The steric demand of the bicyclic structures is considerable because both three-membered rings exhibit acute O−Si−N angles of ca. 45° and thus underlie strong ring tension. It should be noted that the first calculations on dyotropic transition states in silylhydroxylamines were carried out by Müller.[5] Compared to the reactants **A** and **B**, the O−N bonds are only slightly longer by 4.6 and 5.3 pm, respectively. In both transition states, the hydroxylamine Si−O bonds are considerably stretched (by 39.7 pm and 46.1 pm for **TSdA** and **TSdB**, respectively). The original and the newly formed Si−O bonds are almost

Table 2. B3LYP/6-31G(d) geometries of the dyotropic transition states **TSdA** and **TSdB**; bond lengths in pm, angles in °; bond angles are denoted by α, torsional angles by θ

	TSdA	TSdB
r(ON)	154.4	153.0
r(Si′O)	208.2	217.4
r(Si′N)	181.4	180.8
r(Si′′O)	206.5	212.4
r(Si′′N)	188.6	187.8
r(NSi)	183.5	180.2
α(OSi′N)	46.0	44.0
α(OSi′′N)	45.7	44.4
α(Si′NSi)	118.7	118.4
θ(Si′ONSi′′)	122.1	123.3
θ(Si′ONSi)	115.6	117.0

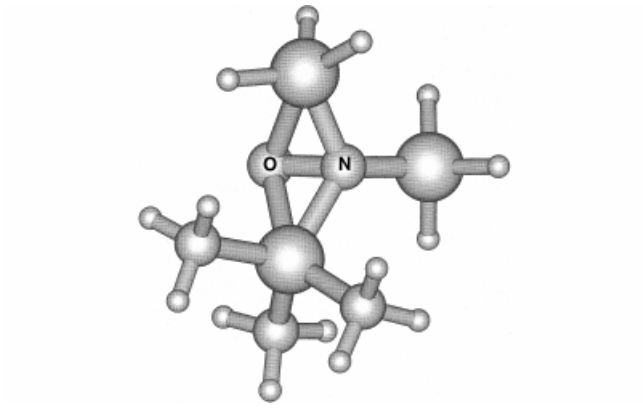

Figure 1. Structure of saddle point **TSdB** (bicyclic dyotropic transition state; see text for details)

equal in length. On the contrary, the hydroxylamine Si−N bonds are stretched by only ca. 10 pm, and the newly formed endocyclic Si−N bond lengths are 7 pm longer that the original ones. The exocyclic Si−N bond is slightly elongated in the dyotropic TS compared to the Si−N bonds in hydroxylamines. The angle between the two three-membered rings is given by the torsional angle $\theta(Si_1ONSi_2)$, which is calculated to be 122 and 123° in **TSdA** and **TSdB**, respectively. The geometries are in very good agreement with the results for $H_3SiO-N(SiH_3)_2$ reported in ref.[5]

In Table 3, the equilibrium structures of the eight silylaminodisiloxanes **PA**, **PA1**, **PB**, **PB1**, **PC1**, **PC2**, **PD1**, and **PD2** are given. These structures may be compared with the structures of the diazasilacyclopropanes discussed in refs.[17,18] The triangular O−Si−N structural motif is analogous to the SiN_2 ring; however, the N−O bond is broken (distance 272 to 286 pm) and the nitrogen atom bears an additional substituent. The O−Si bonds are considerably shortened compared to those in the hydroxylamines, on average by 4 pm. The shortest O−Si bond length is calculated to be only 162 pm. The Si−N bonds are also slightly shorter in the disiloxanes, but the effect is less pronounced compared to the situation with the Si−O bonds. The central silicon atom is clearly sp^3-hybridised (as is the case for the diazasilacyclopropanes[17,18]). The Si−O−Si angles, however, are between 138 and 153°, and indicate sp^2 hybridisation of the oxygen atom with a tendency towards sp hybridisation. The Si−N−Si angles are in the range 124 to 132°. The sum of the angles at the nitrogen centre amounts to almost 360° throughout, clearly indicating sp^2 hybridisation.

Table 3. B3LYP/6-31G(d) equilibrium geometries of the silylaminodisiloxanes (products **PA**, **PA1**, **PB**, **PB1**, **PC1**, **PC2**, **PD1**, and **PD2**); bond lengths in pm, angles in °; bond angles are denoted by α, torsional angles by θ; R = H for **PA1**, **PB** and **PC2**; R = Me otherwise values in parentheses give the equilibrium geometry of structure **PB** obtained at the B3LYP/6-31+G(d) level of theory

	PA	PA1	PB	PB1	PC1	PC2	PD1	PD2
r(SiO)	164.4	166.7	166.8 (166.3)	164.9	167.9	167.0	168.0	169.1
r(OSi)	167.6	165.1	164.4 (163.9)	167.2	163.9	164.5	163.8	162.1
r(SiN)	174.3	173.1	173.9 (173.9)	174.9	172.8	174.0	174.0	170.3
r(NSi)	176.9	176.3	174.4 (174.7)	174.3	174.6	173.7	171.8	175.0
r(NO)	278.7	285.8	285.6 (283.9)	280.6	272.4	283.6	271.7	275.7
r(NR)	147.8	101.7	101.6 (101.7)	148.0	147.9	101.8	148.4	148.4
α(SiOSi)	148.9	150.3	153.3 (178.4)	144.3	142.5	150.6	142.2	138.3
α(OSiN)	109.2	115.3	115.1 (114.3)	110.2	107.9	113.8	107.0	112.1
α(SiNSi)	126.0	131.8	129.1 (129.2)	128.5	124.6	130.8	123.8	126.0
θ(SiOSiN)	179.2	65.8	40.3 (174.8)	49.5	148.2	58.4	146.5	154.1
θ(OSiNSi)	55.8	78.1	83.8 (84.1)	113.0	170.1	115.0	175.6	35.3

Table 4. B3LYP/6-31G(d) equilibrium geometries of the transition states for Si insertion into the N−O bond (**TSA**, **TSA1**, **TSB**, **TSB1**, **TSC1**, **TSC2**, **TSD1** and **TSD2**); bond lengths in pm, angles in °; bond angles are denoted by α, torsional angles by θ; R = H for **TSA1**, **TSB** and **TSC2**; R = Me otherwise; values in parentheses give the equilibrium geometry of structure **TSB** obtained at the B3LYP/6-31+G(d) level of theory

	TSA	TSA1	TSB	TSB1	TSC1	TSC2	TSD1	TSD2
r(SiO)	166.3	169.7	169.9 (170.4)	166.6	169.9	170.2	170.5	169.1
r(OSi)	192.1	183.0	182.4 (183.5)	193.2	183.6	181.8	185.3	176.7
r(SiN)	170.5	171.6	171.5 (171.6)	170.5	170.0	170.4	168.6	169.1
r(NSi)	178.0	178.8	177.1 (177.4)	176.7	176.4	176.5	174.8	177.9
r(NO)	206.4	207.1	205.2 (205.5)	204.6	205.6	206.7	203.2	211.9
r(SiR)	208.4	160.5	161.0 (160.9)	209.8	206.1	162.2	207.3	202.0
r(NR)	248.0	212.7	210.5 (210.3)	245.4	248.5	208.4	245.6	247.4
α(SiOSi)	135.8	134.7	141.6 (138.9)	137.7	135.3	137.7	135.9	139.9
α(OSiN)	69.1	71.4	70.8 (70.7)	68.1	71.0	71.8	69.9	75.5
α(SiNSi)	139.7	131.6	131.0 (131.9)	131.2	133.8	136.5	137.1	133.9
θ(SiOSiN)	94.2	100.8	100.8 (97.7)	87.8	99.5	92.2	95.6	111.4
θ(OSiNSi)	89.5	92.7	88.0 (89.5)	87.8	90.3	89.7	84.2	84.3

Table 4 gives the geometrical parameters of the saddle points corresponding to transition states **TSA**, **TSA1**, **TSB**, **TSB1**, **TSC1**, **TSC2**, **TSD1**, and **TSD2**. As an example, the structure **TSC1** is shown graphically in Figure 2. The O−N bonds (between 203 and 212 pm) are markedly elongated (by more than 30 pm) compared with the corresponding bonds in the reactant structures. The exocyclic Si−O bond length is only slightly greater than the corresponding bond length in the products. The newly formed O−Si bond is relatively long (up to 20 pm longer than that in the silylaminodisiloxanes). The exocyclic N−Si bond length is slightly greater than the corresponding bond length in the product. The Si−N bond bridging to the oxygen atom is only slightly shorter than that in the silylaminodisiloxanes, and much shorter than that in the hydroxylamines. The acute central

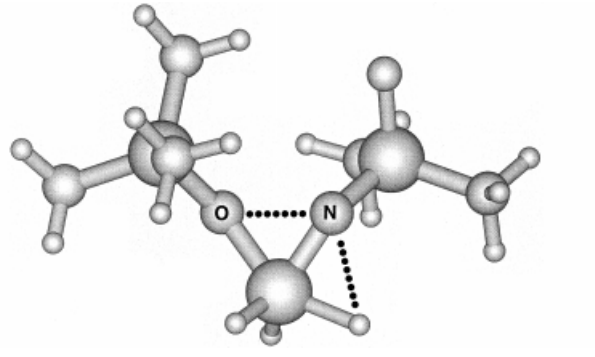

Figure 2. Structure of the saddle point **TSC1** (SiH_3 insertion into the O−N bond; see text for details)

O−Si−N angle is between 68 and 76°. The Si−O−Si and Si−N−Si angles are between 131 and 142°.

The transition states are bicyclic structures with the first ring formed by the NO moiety and the inserting silicon atom, while the second ring is formed by the central silicon atom, the nitrogen atom, and the group R transferred from the silicon atom to the nitrogen atom (see Figure 2). The transferred group (R) is either a hydrogen atom or a methyl group. The silicon, the oxygen, the nitrogen, and the hydrogen atom (or the methyl carbon atom) are almost coplanar. At the saddle point, the reacting Si−R bonds are considerably stretched. Thus, the reacting Si−C bond in **TSA** is 19.2 pm longer than the other two Si−C bonds (198.2 pm) at the same silicon atom. The Si−H bond in **TSA1** is 11.7 pm longer compared to the other two Si−H bond lengths (148.8 pm). However, the new bond to the nitrogen atom has yet to be formed at the saddle point. The N−C distance in **TSA** is 248.0 pm and the N−H distance in **TSA1** amounts to 212.7 pm; these are much longer than the corresponding distances in the silylaminodisiloxanes (Table 3). Thus, the saddle points reported in Table 4 may be classified as *early* transition states. The N−O bond is not yet fully broken and the interaction between the nitrogen atom and the transferred moiety is only weak. The bicyclic first-order saddle point structures for silicon insertion into the N−O bond are analogous to the dyotropic transition states **TSdA** and **TSdB** (the bond between the central silicon atom and the nitrogen atom adopts the role of the N−O bond in the dyotropic TS). The B3LYP/6-31G(d) structures of all compounds described in this quantum chemical study can be obtained from one of the authors (sschmat@gwdg.de).

The influence of diffuse basis functions [6-31+G(d) basis set] on the geometries of the stationary points was investigated for structures **B**, **PB**, and **TSB** (see Tables 1, 3, and 4). The only remarkable deviation from the B3LYP/6-31G(d) results was found for the Si−O−Si angle in the silylaminodisiloxane **PB**, which is widened by 25°. The Si−O−Si unit becomes almost linear (178.4°) when the additional diffuse functions are taken into account. However, the energetics are hardly affected. The saddle point **TSB** is found at 38.3 kcal·mol^{-1} above **B** [38.2 kcal·mol^{-1} with 6-31G(d)], whereas the product **PB** is located at 84.9 kcal·mol^{-1} below **B** [83.8 kcal·mol^{-1} with 6-31G(d)].

Energetics

In Table 5, the energetics of the dyotropic transition state **TSdA** and silylhydroxylamine **A1** relative to species **A** are given. **A1** is more stable than **A** by ca. 3 kcal·mol^{-1}, and zero-point energy effects enhance its stability. Energetically, the dyotropic TS is located at 33 kcal·mol^{-1} above the reactant. This is of the same order of magnitude as reported by Wolfgramm et al.[5] The dyotropic **TSdB** is calculated to be 36 kcal·mol^{-1} above the reactant **B** (Table 6). The isomer **B1** is 1.5 kcal·mol^{-1} higher in energy than **B**. This indicates that configurations with silyl groups at the nitrogen atom and trimethylsilyl groups at the oxygen site are energetically favoured.

In Figures 3−6, the potential energy profiles of the isomerising tris(silyl)hydroxylamines **A**, **B**, **C**, and **D** are displayed graphically as functions of the reaction coordinate. Note that the stationary points are connected by a smooth curve; the "reaction coordinate" in Figures 3−6 does not have any quantitative physical significance. The influence of zero-point vibrational energy (at the harmonic level; reaction coordinate at saddle points not included) is given in Tables 5−8. The effect of finite temperature (298 K) is also highlighted in these tables (reaction enthalpies $\Delta_R H°$). As can be seen from Figure 3, the insertion of an SiH_3 group into the N−O bond is favoured compared to $SiMe_2$ insertion. In addition to the thermodynamic control ($|\Delta E_{\mathbf{PA1}}| > |\Delta E_{\mathbf{PA}}|$), the reaction is also kinetically controlled (by the barriers to isomerisation $\Delta E_{\mathbf{TSA1}} < \Delta E_{\mathbf{TSA}}$). Silylhydroxylamine **A** first has to undergo isomerisation via the dyotropic transition state **TSdA**, for which the activation energy (barrier height $\Delta E_{\mathbf{TSdA}}$) is very similar to the corresponding value for the silyl group insertion ($\Delta E_{\mathbf{TSA1}}$). The larger reaction enthalpy and the lower isomerisation barrier determine the course of the reaction (**A** → **PA1**).

A similar conclusion can be drawn from Figure 4. Here, reaction **B** → **PB** (SiH_3 insertion) is favoured both thermodynamically and kinetically. The barrier $\Delta E_{\mathbf{TSdB}}$ for the dyotropic rearrangement **B** → **B1** is smaller than the barrier $\Delta E_{\mathbf{TSB1}}$ for $SiMe_3$ insertion **B1** → **PB1**.

In Figure 5, insertion of a silyl group is compared with that of a fluorodimethylsilyl group. Again, SiH_3 insertion (**C** → **PC1**) is favoured both thermodynamically and kinetically (Table 7).

Table 5. Energetics of the reactions involving tris(silyl)hydroxylamine **A** (energies in kcal·mol^{-1} with respect to the starting material); E_{zp} denotes the zero-point energy contribution

		A	**TSdA**	**A1**	**TSA1**	**PA1**	**TSA**	**PA**
ΔE	B3LYP/6-31G(d)	0.0	31.2	−2.6	31.7	−87.7	41.2	−65.9
$\Delta(E+E_{zp})$	B3LYP/6-31G(d)	0.0	30.7	−2.9	29.2	−86.1	39.1	−64.5
$\Delta_R H°$(298 K)	B3LYP/6-31G(d)	0.0		−2.8		−85.7		−64.3
ΔE	B3LYP/6-311+G(2d,p)[a]	0.0	32.8	−2.6	30.9	−91.7	40.0	−66.1
ΔE	MP2/6-31G(d)[a]	0.0	26.5	−1.1	48.4	−90.0	55.9	−69.6
ΔE	MP2/6-31+G(d,p)[a]	0.0	26.6	−0.7	50.2	−90.9	55.3	−69.2

[a] At B3LYP/6-31G(d) geometry.

Table 6. Energetics of the reactions involving tris(silyl)hydroxylamine **B** (energies in kcal·mol^{-1} with respect to the starting material); E_{zp} denotes the zero-point energy contribution

		B	TSdB	B1	TSB1	PB1	TSB	PB
ΔE	B3LYP/6-31G(d)	0.0	35.7	1.5	46.4	−65.1	38.2	−83.8
$\Delta(E+E_{zp})$	B3LYP/6-31G(d)	0.0	35.3	1.5	44.5	−63.5	35.9	−81.8
$\Delta_R H°$(298 K)	B3LYP/6-31G(d)	0.0		1.5		−63.3		−81.5
ΔE	B3LYP/6-311+G(2d,p)[a]	0.0	35.7	1.3	44.6	−65.5	36.9	−87.6
ΔE	MP2/6-31G(d)[a]	0.0	30.8	0.4	58.3	−70.2	53.1	−88.5
ΔE	MP2/6-31+G(d,p)[a]	0.0	30.4	0.2	57.4	−70.0	53.8	−89.8

[a] At B3LYP/6-31G(d) geometry.

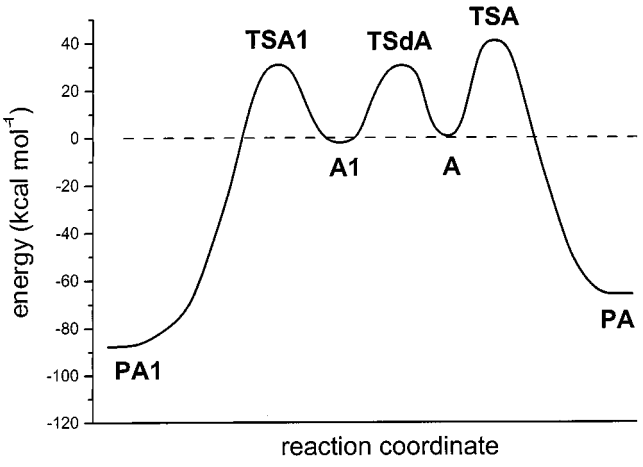

Figure 3. Potential energy diagram for reaction **A** (schematic)

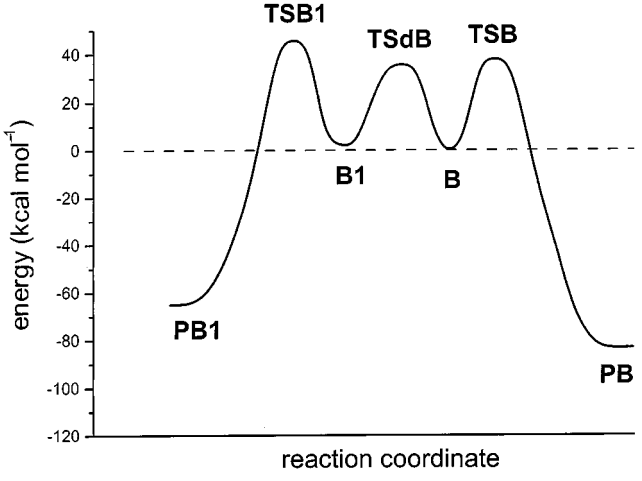

Figure 4. Potential energy diagram for reaction **B** (schematic)

Figure 6 shows the thermal rearrangement of *N*-(difluoromethyl)-*N*-(fluorodimethylsilyl)-*O*-(trimethylsilyl)-hydroxylamine. Insertion of the difluorosilyl group has a slightly smaller associated barrier height ΔE_{TSD1} than insertion of the monofluorosilyl group. However, the product **PD2** is energetically favoured by 1.3 kcal·mol^{-1} (Table 8). The reaction is clearly subject to thermodynamic control. This is in keeping with the conditions of preparation of the silylaminodisiloxane, i.e. heating of a fluoro-substituted tris(silyl)hydroxylamine up to 200 °C and keeping it at this temperature for several hours.

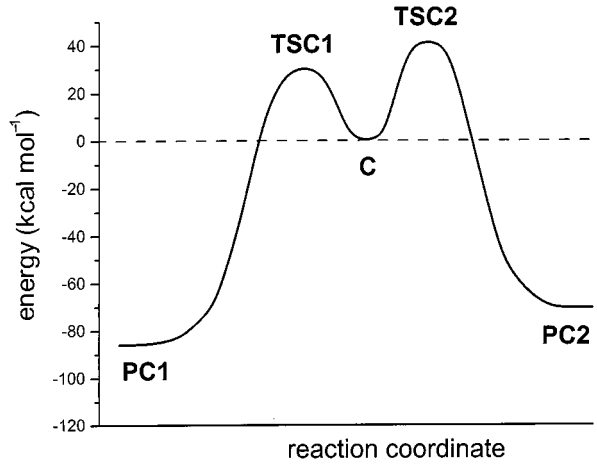

Figure 5. Potential energy diagram for reaction **C** (schematic)

It should be noted that the theoretical results are in nice agreement with the experimental finding that during the conversion of **1** to **4** a structural isomer of **1** was monitored. This isomer is formed by a dyotropic rearrangement. After this step, the $SiHMe_2$ group inserts instead of the $SiMe_3$ group.

It remains to be considered how well hybrid DFT methods, e.g. B3LYP, can predict transition-state geometries and barrier heights. Hybrid DFT involves mixing various amounts of the Hartree−Fock non-local exchange operator with DFT exchange-correlation functionals, and it has been observed that the fraction needed for an accurate prediction of thermochemical data differs from the optimal fraction for predicting accurate barrier heights. Recently, Lynch and Truhlar[22] reported DFT calculations of barrier heights in 22 reactions and found a mean unsigned error of 3.4−4.2 kcal·mol^{-1} (depending on the basis set) in comparison with best estimates derived from experimental data. Møller−Plesset second-order perturbation theory (MP2) performed slightly less well. Lynch and Truhlar recommend their own hybrid method MPW1K,[23] which gave a mean unsigned error of only 1.5 kcal·mol^{-1}. However, all of the 22 reactions involve free radicals and the transfer of a hydrogen atom, and all but one are bimolecular reactions. Since the empirical data are as yet only limited, and since, in the present work, we focus on the energetic *differences* between several reaction pathways, we are confident that the B3LYP method yields reliable results.

Table 7. Energetics of the reactions involving tris(silyl)hydroxylamine **C** (energies in kcal·mol^{-1} with respect to the starting material); E_{zp} denotes the zero-point energy contribution

		C	TSC1	PC1	TSC2	PC2
ΔE	B3LYP/6-31G(d)	0.0	36.4	−85.9	41.7	−70.4
$\Delta(E+E_{zp})$	B3LYP/6-31G(d)	0.0	34.0	−83.6	39.5	−68.8
$\Delta_R H°$(298 K)	B3LYP/6-31G(d)	0.0		−83.5		−68.7
ΔE	B3LYP/6-311+G(2d,p)[a]	0.0	35.0	−90.1	41.6	−70.8
ΔE	MP2/6-31G(d)[a]	0.0	51.1	−90.3	55.7	−74.6
ΔE	MP2/6-31+G(d,p)[a]	0.0	51.6	−91.6	56.0	−73.8

[a] At B3LYP/6-31G(d) geometry.

Table 8. Energetics of the reactions involving tris(silyl)hydroxylamine **D** (energies in kcal·mol^{-1} with respect to the starting material); E_{zp} denotes the zero-point energy contribution

		D	TSD1	PD1	TSD2	PD2
ΔE	B3LYP/6-31G(d)	0.0	43.5	−68.6	45.6	−69.9
$\Delta(E+E_{zp})$	B3LYP/6-31G(d)	0.0	41.6	−66.7	43.7	−68.0
$\Delta_R H°$(298 K)	B3LYP/6-31G(d)	0.0		−66.8		−68.1
ΔE	B3LYP/6-311+G(2d,p)[a]	0.0	43.0	−69.2	45.2	−71.1
ΔE	MP2/6-31G(d)[a]	0.0	59.6	−71.9	57.6	−74.1
ΔE	MP2/6-31+G(d,p)[a]	0.0	60.0	−71.0	57.6	−73.3

[a] At B3LYP/6-31G(d) geometry.

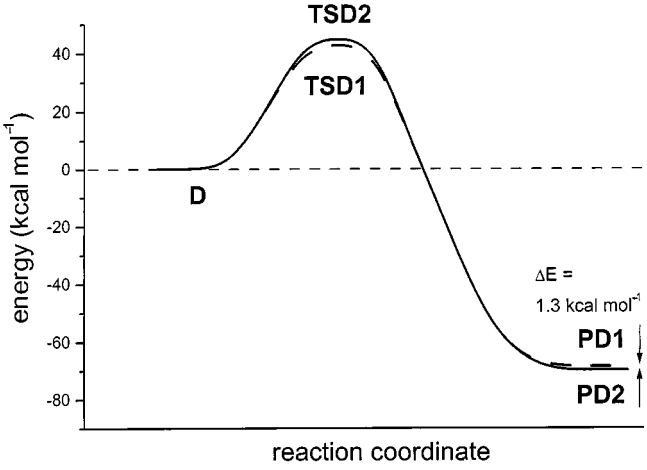

Figure 6. Potential energy diagram for reaction **D** (schematic)

In order to study the influence of polarization and diffuse basis functions on the energetics of the four systems, we performed B3LYP/6-311+G(2d,p) calculations on the B3LYP/6-31G(d) geometries (see Tables 5−8). Overall, the results are in good agreement with those obtained employing the smaller basis set. The products **PA1**, **PB**, and **PC1** are lowered in energy because the additional diffuse and polarization functions allow for a better description of the SiH_2−NH unit in these cases.

We also carried out MP2 calculations with the 6-31G(d) and 6-31+G(d,p) basis sets at the optimized B3LYP geometries (see Tables 5−8). The energetic differences between reactants and products are very close to the DFT results. The two saddle points describing the dyotropic transition states are slightly lower in energy than the corresponding saddle points from the MP2 calculations. However, all other MP2 saddle points are much higher in energy. This can be explained by the fact that the dyotropic transition states (TS) can be classified as "tight" TS, whereas the other TS (Table 4) are "loose" TS with considerably stretched bonds. MP2 does not include a major fraction of the non-dynamical correlation energy and is not capable of describing such loose structures. In particular, the order of the two saddle points in reaction according to eq. 13 is reversed at the MP2 level of theory.

Normal Modes of Transition States

The harmonic vibrational frequencies ω_{TS} of the reactive normal modes Q_{TS} at the various saddle points are given in Table 9. The two dyotropic transition states have rather similar imaginary frequencies and corresponding reduced masses μ_{TS}. In both cases, a silyl group and a trimethylsilyl group undergo simultaneous migration. However, the motion along Q_{TS} is governed by the oxygen atom, which is much lighter than the heavy silyl groups (see Figure 7). From the viewpoint of reaction dynamics, the term "silyl group migration" is somewhat misleading.

Table 9. Harmonic vibrational frequencies in cm^{-1} of the reactive normal coordinates Q_{TS} of the transition states; the corresponding reduced mass in a.m.u. is denoted by μ_{TS}

	TSdA	TSA	TSA1	TSdB	TSB	TSB1	TSC1	TSC2	TSD1	TSD2
ω_{TS}	278*i*	558*i*	505*i*	267*i*	559*i*	617*i*	613*i*	527*i*	509*i*	546*i*
μ_{TS}	8.96	2.78	8.46	8.04	7.04	2.48	2.40	7.04	8.99	8.80

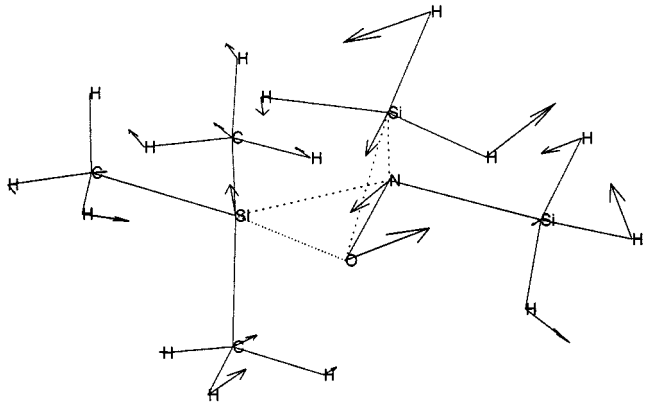

Figure 7. The reaction coordinate Q_{TS} at the saddle point **TSdB**, i.e. the normal coordinate of the mode with the imaginary vibrational frequency ω_{TS}

The transition states for SiH_3 group insertion into the N−O bond (**TSA**, **TSB1**, and **TSC1**) exhibit very similar characteristic ω_{TS} and μ_{TS} data for the reactive normal modes Q_{TS}. Inspection of the remaining saddle points (**TSA1**, **TSB**, **TSC2**, **TSD1**, and **TSD2**) reveals that substitution of an $SiMe_3$ group by $SiMe_2F$ or $SiMeF_2$ has only a small influence on the nuclear dynamics in the saddle-point region of the PES (the curvature of the saddle point, given by $\mu_{TS}\,\omega_{TS}^2$, is relatively similar). The reactive motion is described by the fission of the N−O bond and the insertion of the silicon atom (see Figure 8). The bond between the transferred group (H or CH_3) is considerably stretched. The nitrogen atom moves towards the transferred group and forms a new bond.

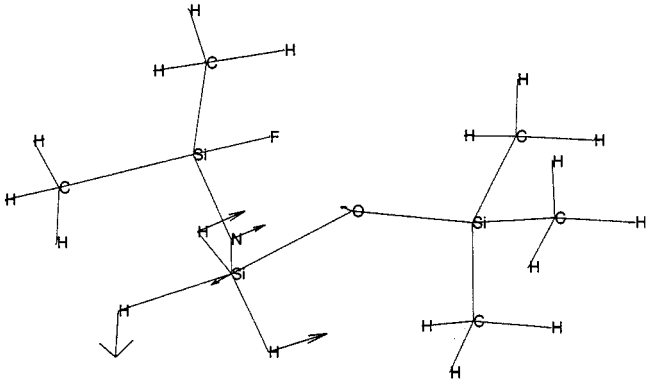

Figure 8. The reaction coordinate Q_{TS} at the saddle point **TSC2**, i.e. the normal coordinate of the mode with the imaginary vibrational frequency ω_{TS}

In summary, it has been shown that the insertion of a silyl group into the N−O bond is energetically favoured if it occurs from the nitrogen atom. Furthermore, a monofluorosilyl group inserts into the N−O bond whereas the difluorosilyl group does not. Insertion of SiH_2 stabilises the product by 86 kcal·mol^{-1} whereas insertion of $SiMe_2$, SiMeF, or SiF_2 yields a stabilisation of 66, 70, and 69 kcal·mol^{-1}, respectively. The transition state for SiH_2 insertion is located at 35±3 kcal·mol^{-1} above the tris(silyl)hydroxylamines, whereas the transition state for insertion of $SiMe_2$, SiMeF, and SiF_2 is ca. 10 kcal·mol^{-1} higher (44±3 kcal·mol^{-1}).

Experimental Section

General: All experiments were performed in oven-dried glassware using standard inert gas and vacuum-line techniques. NMR spectra were recorded from samples in $CDCl_3$ with $SiMe_4$ and C_6F_6 (^{1}H, ^{13}C, ^{19}F, ^{29}Si) as internal and $MeNO_2$ (^{15}N) as external references. Mass spectral data are reported in mass-to-charge units (*m*/*z*). The progress of the reactions was monitored by ^{19}F NMR spectroscopy. The compounds were obtained in analytically pure form.

***O*-(Dimethylsilyl)-*N*,*N*-bis(trimethylsilyl)hydroxylamine (1):** To a solution of *N*,*N*-bis(trimethylsilyl)hydroxylamine (8.8 g, 0.05 mol) in *n*-hexane (70 mL), *n*BuLi (1.6 M solution in *n*-hexane, 0.05 mol) was slowly added. After heating under reflux for 2 h, the reaction mixture was cooled to room temperature, whereupon $ClSiMe_2H$ (0.05 mol, 4.7 g) was added. LiCl was removed on a frit and **1** was purified by distillation; yield 73%; b.p. 63 °C/0.01 mbar. ^{1}H NMR ($CDCl_3$): δ = 0.11 [s, 18 H, $Si(CH_3)_3$], 0.22 [d, $^3J_{H,H}$ = 2.9 Hz, 6 H, $Si(CH_3)_2$], 4.7 (sept, $^3J_{H,H}$ = 2.9 Hz, 1 H, SiH). ^{13}C NMR ($CDCl_3$): δ = −1.22 (SiC_3), 0.76 (SiC_2). ^{29}Si NMR ($CDCl_3$): δ = 8.27 [$Si(CH_3)_3$], 13.43 (SiH). MS (EI): *m*/*z* (%) = 235(21) $[M]^+$, 220(8) $[M - CH_3]^+$. IR: $\tilde{\nu}$ = 2131.6 cm^{-1} (SiH). $C_8H_{25}NOSi_3$ (235.55): calcd. C 40.79, H 10.70; found C 40.53, H 10.32.

***N*,*N*-Bis(*tert*-butyldimethylsilyl)-*O*-(difluorophenylsilyl)hydroxylamine (2):** F_3SiPh (8.1 g, 0.05 mol) was added to *N*,*N*-bis(*tert*-butyldimethylsilyl)-*O*-lithiohydroxylamine[6] (13.0 g, 0.5 mol) at 0 °C and the mixture was slowly allowed to warm to room temperature. **2** was freed of LiF by centrifugation; yield 76%; b.p. 100 °C/0.05 mbar. ^{1}H NMR ($CDCl_3$): δ = 0.23 (t, $^6J_{HF}$ = 0.56 Hz, 12 H, $NSiCH_3$), 1.01 [s, 18 H, $NSiC(CH_3)_3$], 7.0−7.2 (C_6H_5). ^{13}C NMR ($CDCl_3$): δ = −2.91 (t, $^5J_{C,F}$ = 1.51 Hz, NSiC), 20.03 ($NSiCC_3$), 27.89 ($NSiCC_3$), 125.04 (t, $^2J_{C,F}$ = 26.7 Hz, C-1 of Ph), 128.47 (t, $^4J_{C,F}$ = 0.7 Hz, C-3,5 of Ph), 132.25 (C-4 of Ph), 134.72 (t, $^3J_{C,F}$ = 119 Hz, C-2,6 of Ph). ^{19}F NMR ($CDCl_3/C_6F_6$): δ = 29.5. ^{29}Si NMR ($CDCl_3$): δ = −65.02 (t, J_{SiF} = 278.7 Hz, OSiF), 14.85 (NSi). MS (EI): *m*/*z* (%) = 388(8) $[M - CH_3]^+$, 346(100) $[M - C(CH_3)_3]^+$.

***N*,*O*-Bis(*tert*-butyldimethylsilyl)-*N*-(difluorophenylsilyl)hydroxylamine (3):** A solution of **2** (20.2 g, 0.05 mol) in THF (50 mL) was refluxed for 3 d (^{19}F NMR control). Thereafter, the **3** obtained was distilled in vacuo. yield 67%. ^{1}H NMR ($CDCl_3$): δ = 0.12 (s, 6 H, $OSiCH_3$), 0.16 (s, 6 H, $NSiCH_3$), 0.28 [s, 9 H, $OSiC(CH_3)_3$], 0.88 [s, 9 H, $NSiC(CH_3)_3$], 7.2−7.8 (m, 5 H, C_6H_5). ^{13}C NMR ($CDCl_3$): δ = −6.37 ($NSiCH_3$), −5.49 ($OSiCH_3$), 17.82 [$NSiC(CH_3)_3$], 18.12 [$OSiC(CH_3)_3$], 25.84 [$NSiC(CH_3)_3$], 26.39 [$OSiC(CH_3)_3$]. ^{19}F NMR ($CDCl_3$): δ = 27.19 (OSiF). ^{29}Si NMR ($CDCl_3$): δ = −51.02 (t, $^1J_{SiF}$ = 271.19 Hz, NSiF), 15.49 (NSi), 24.56 (OSi). MS (EI): *m*/*z* (%) = 403(2) $[M]^+$, 388(8) $[M - CH_3]^+$, 346(100) $[M - CMe_3]^+$. $C_{18}H_{35}F_2NOSi_3$ (403.20): calcd. C 53.62, H 8.75; found C 53.16, H 8.49.

Compounds 4 and 5: The respective tris(silyl)hydroxylamine **1** or **3** (0.03 mol) was heated under reflux without a solvent for 3 d. Compounds **4** and **5** produced were purified by distillation in vacuo.

1,1,1,3,3-Pentamethyl-3-[(trimethylsilyl)amino]-1,3-disiloxane (4): Yield 82%; b.p. 63 °C/10 mbar. ^{1}H NMR ($CDCl_3$): δ = 0.04

[$Si(CH_3)_2$], 0.06 [$NSi(CH_3)_3$], 0.07 [$OSi(CH_3)_3$], 0.42 (NH). ^{13}C NMR ($CDCl_3$): δ = 1.97 [$OSi(CH_3)_3$], 2.30 [$NSi(CH_3)_3$], 2.46 [$Si(CH_3)_2$]. ^{15}N NMR ($CDCl_3$): δ = −344.71 (NH). ^{29}Si NMR ($CDCl_3$): δ = −11.24 (NSi), 2.12 (OSiN), 6.08 (SiO). MS (EI): *m*/*z* (%) = 235(4) $[M]^+$, 220(100) $[M - CH_3]^+$. $C_8H_{25}NOSi_3$ (235.55): calcd. C 40.79, H 10.70; found C 40.31, H 10.35.

1,3-Di-*tert*-butyl-3-[(difluorophenylsilyl)methylamino]-1,1,3-trimethyl-1,3-disiloxane (5): Yield 67%; b.p. 101 °C/0.05 mbar. ^1H NMR ($CDCl_3$): δ = 0.14 (3 H, $OSiCH_3$), 0.15 (3 H, $OSiCH_3$), 0.36 (3 H, $SiCH_3$), 0.97 [9 H, $SiC(CH_3)_3$], 1.04 [9 H, $SiC(CH_3)_3$], 2.68 (t, $^4J_{HF}$ = 1.15 Hz, 9 H, NCH_3), 7.4−7.8 (m, 5 H, C_6H_5). ^{13}C NMR ($CDCl_3$): δ = −2.92 ($OSiCH_3$), −2.90 ($OSiCH_3$), −5.66 (t, $^4J_{HF}$ = 2.53 Hz, $SiCH_3$), 18.27 [$SiC(CH_3)_3$], 18.37 [$SiC(CH_3)_3$], 25.84 [$SiC(CH_3)_3$], 26.67 [$SiC(CH_3)_3$], 33.72 (t, $^3J_{C,F}$ = 2.45 Hz, NCH_3), 128.04 (C-1 of Ph), 128.27 (C-3,5 of Ph), 131.57 (C-4 of Ph), 134.72 (t, $^3J_{C,F}$ = 1.26 Hz, C-2,6 of Ph). ^{19}F NMR ($CDCl_3$): δ = 24.71−26.55 (NSiF). ^{29}Si NMR ($CDCl_3$): δ = −47.22 (t, $^1J_{SiF}$ = 268.35 Hz, NSiF), 8.95 (t, $^3J_{SiF}$ = 1.53 Hz, NSiO), 11.62 (OSi). MS (EI): *m*/*z* (%) = 403(2) $[M]^+$, 388(8) $[M - CH_3]^+$, 346(100) $[M - CMe_3]^+$. $C_{18}H_{35}F_2NOSi_3$ (403.20): calcd. C 53.62, H 8.75; found C 53.74, H 8.92.

Acknowledgments

S. S. is indebted to Professor Peter Botschwina for continuous support. We would like to thank Dr. Rainer Oswald for his help with Figures 7 and 8. Helpful discussions with Dr. Thomas Müller (University of Frankfurt/Main) are gratefully acknowledged. Most of the calculations were carried out on workstations of the Gesellschaft für wissenschaftliche Datenverarbeitung Göttingen (GWDG). Support through Sonderforschungsbereich 357 "Molekulare Mechanismen unimolekularer Prozesse" is gratefully acknowledged. We are grateful to the Deutsche Forschungsgemeinschaft and Fonds der Chemischen Industrie for support of this work.

[1] P. Boudjouk, R. West, *Intra-Sci. Chem. Rep.* **1973**, *7*, 65.
[2] R. West, *Adv. Organomet. Chem.* **1977**, *16*, 1.
[3] R. Wolfgramm, U. Klingebiel, *Z. Anorg. Allg. Chem.* **1998**, *624*, 1031.
[4] R. Wolfgramm, U. Klingebiel, M. Noltemeyer, *Z. Anorg. Allg. Chem.* **1998**, *624*, 865.
[5] R. Wolfgramm, T. Müller, U. Klingebiel, *Organometallics* **1998**, *17*, 3222.
[6] F. Diedrich, U. Klingebiel, M. Schäfer, *J. Organomet. Chem.* **1999**, *588*, 242.
[7] F. Diedrich, U. Klingebiel, F. Dall′Antonia, C. Lehmann, M. Noltemeyer, T. R. Schneider, *Organometallics* **2000**, *19*, 5376.
[8] R. West, P. Boudjouk, T. A. Matuszko, *J. Am. Chem. Soc.* **1969**, *91*, 5184.
[9] E. Frainnet, F. Duboudin, F. Dabescat, G. C. Vincon, *C. R. Acad. Sci., Ser. C* **1973**, *276*, 1469.
[10] C. Trindle, D. D. Schillady, *J. Am. Chem. Soc.* **1973**, *95*, 703.
[11] M. T. Reetz, *Adv. Organomet. Chem.* **1977**, *16*, 33−65.
[12] R. Wolfgramm, U. Klingebiel, *Z. Anorg. Allg. Chem.* **1998**, *624*, 1035−1040.
[13] M. J. Frisch, G. W. Trucks, H. B. Schlegel, G. E. Scuseria, M. A. Robb, J. R. Cheeseman, V. G. Zakrzewski, J. A. Montgomery, R. E. Stratmann, J. C. Burant, S. Dapprich, J. M. Millam, A. D. Daniels, K. N. Kudin, M. C. Strain, O. Farkas, J. Tomasi, V. Barone, M. Cossi, R. Cammi, B. Mennucci, C. Pomelli, C. Adamo, S. Clifford, J. Ochterski, G. A. Petersson, P. Y. Ayala, Q. Cui, K. Morokuma, D. K. Malick, A. D. Rabuck, K. Raghavachari, J. B. Foresman, J. Cioslowski, J. V. Ortiz, A. G. Baboul, B. B. Stefanov, G. Liu, A. Liashenko, P. Piskorz, I. Komaromi, R. Gomberts, R. L. Martin, D. J. Fox, T. Keith, M. A. Al-Laham, C. Y. Peng, A. Nanayakkara, C. Gonzales, M. Challacombe, P. M. W. Gill, B. Johnson, W. Chen, M. W. Wong, J. L. Andres, C. Gonzales, M. Head-Gordon, E. S. Replogle, J. A. Pople, *GAUSSIAN-98, Revision A.7*, Gaussian, Inc., Pittsburgh PA, **1998**.
[14] A. D. Becke, *J. Chem. Phys.* **1993**, *98*, 5648.
[15] C. Lee, W. Yang, R. G. Parr, *Phys. Rev. B* **1988**, *37*, 785.
[16] C. Gonzales, H. B. Schlegel, *J. Chem. Phys.* **1989**, *90*, 2154; *J. Chem. Phys.* **1990**, *94*, 5523.
[17] E. Gellermann, U. Klingebiel, M. Noltemeyer, S. Schmatz, *J. Am. Chem. Soc.* **2001**, *123*, 378.
[18] S. Schmatz, *J. Phys. Chem. A* **2001**, *105*, 3875.
[19] U. Klingebiel, S. Schmatz, E. Gellermann, C. Drost, M. Noltemeyer, *Monatsh. Chem.* **2001**, *132*, 1105.
[20] E. Gellermann, U. Klingebiel, T. Pape, F. Dall'Antonia, T. R. Schneider, S. Schmatz, *Z. Anorg. Allg. Chem.* **2001**, *627*, 2581.
[21] S. Schmatz, *Organometallics*, in press.
[22] B. J. Lynch, D. G. Truhlar, *J. Phys. Chem. A* **2001**, *105*, 2936.
[23] B. J. Lynch, P. L. Fast, K. Harris, D. G. Truhlar, *J. Phys. Chem. A* **2000**, *104*, 21.

Received August 6, 2001
[I01298]